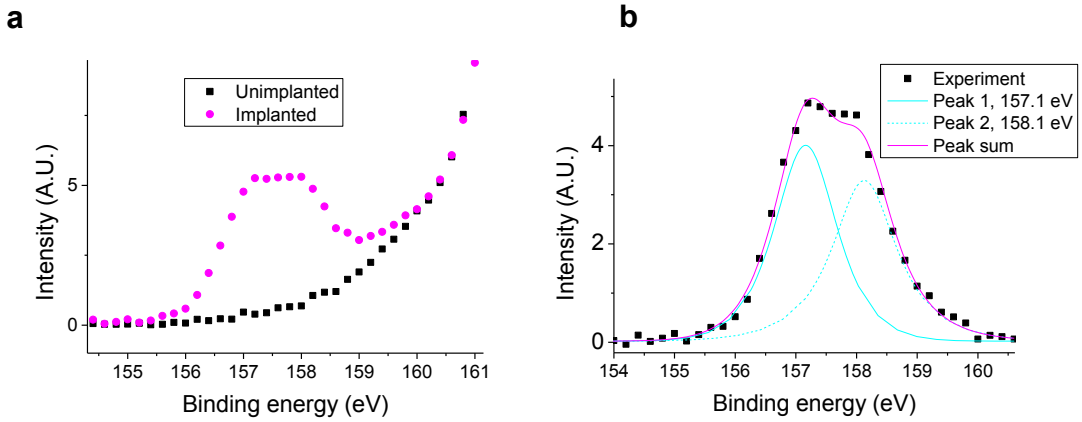

Supplementary Figure 1. (a) The tail of the S 2*p* peak in the unimplanted region was subtracted from the X-ray photoelectron spectroscopy (XPS) spectrum from the implanted region to emphasize the Bi $4f_{7/2}$ peak. (b) XPS spectrum of the Bi $4f_{7/2}$ level in 1×10^{16} ions cm^{-2} Bi-implanted 200 nm thick GaLaSO film, deconvolved into two fitted Gaussian-Lorentzian peaks centred at 157.1 and 158.1 eV.

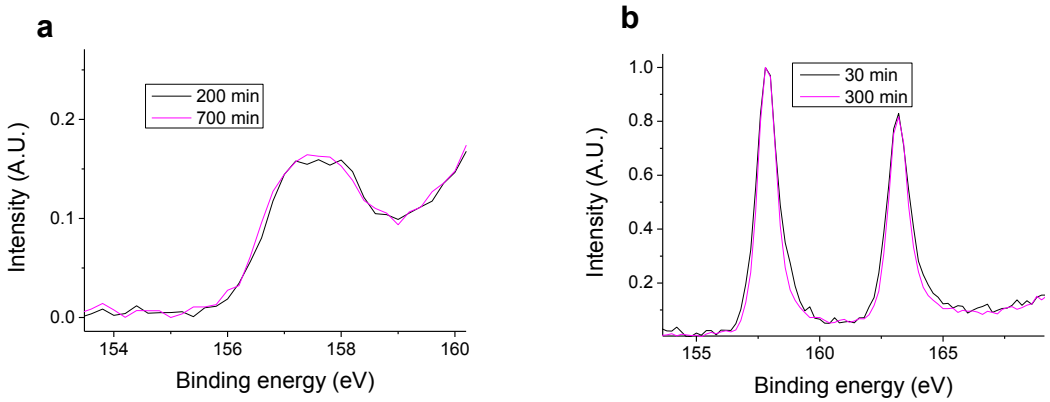

Supplementary Figure 2. X-ray photoelectron spectroscopy (XPS) spectra of the Bi 4*f* level taken at the upper and lower Bi containing etch levels of Bi-implanted GaLaSO (a) and GeTe (b). The total length of X-ray exposure time is indicated for each layer. This shows that X-ray exposure does not change the oxidation state of Bi within our measurement.

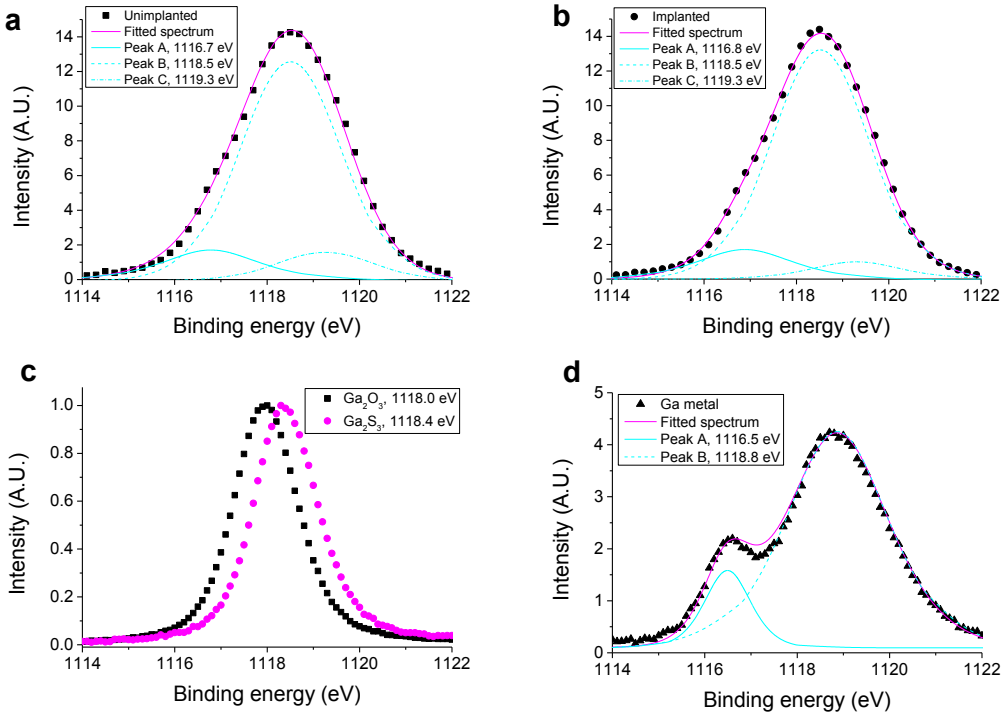

Supplementary Figure 3. Deconvolution into fitted Gaussian-Lorentzian peaks of the X-ray photoelectron spectroscopy (XPS) spectra of the Ga $2p_{3/2}$ level from the unimplanted (a) and implanted (b) regions from a 1×10^{16} ions cm^{-2} Bi-implanted 200 nm thick GaLaSO film. The deconvolution indicates a primary peak (peak B) at 1118.5 eV, with shoulders represented by peaks at 1116.7 eV (peak A) and 1119.3 eV (peak C). It also indicates that the difference between the unimplanted and implanted regions shown in Figure 3 is caused by a decrease in peak C and an increase in peak B after implantation. (c) The XPS spectra of the Ga $2p_{3/2}$ level from Ga_2S_3 and Ga_2O_3 crystalline powders, which peak at 1118.4 and 1118.0 eV, respectively. Ga_2O_3 can exist in various phases; we used the thermodynamically stable monoclinic β-phase. The XPS spectrum of Ga metal is shown in (d); we were unable to sputter off the native oxide due to the low melting temperature of Ga. The spectrum was deconvolved into two peaks at 1116.5 eV and 1118.5 eV, which correspond to Ga metal, and its native oxide.[1,2] Peak A of the GaLaSO film corresponds well in terms of binding energy

with that of Ga metal, indicating that this peak represents Ga-Ga homopolar bonds in the GaLaSO network. Peak B corresponds well with the Ga binding energy of Ga_2S_3 crystalline powder, which suggests that the primary peak (peak B) in the GaLaSO XPS spectra represents an S-coordinated Ga species in a similar configuration to those in Ga_2S_3, ie GaS_4 tetrahedra. After implantation, peak B increases, indicating the formation of GaS_4 tetrahedra; this is also indicated in the Raman spectra in Supplementary Figure 4. The 1119.5 eV binding energy of Ga in a thermally oxidised β-Ga_2O_3 film on GaN[3] corresponds well with peak C in GaLaSO. The large variation in Ga binding energy between bulk β-Ga_2O_3, the native oxide and thermal oxide indicates that the preparation techniques and morphology of gallium oxide can have a significant influence on the Ga binding energy. It is therefore more reasonable to compare the Ga binding energy of our GaLaSO film with Ga_2O_3 in a film morphology, rather than bulk Ga_2O_3. We therefore propose that peak C in the GaLaSO film is due to an O-coordinated Ga species and this Ga species decreases after implantation.

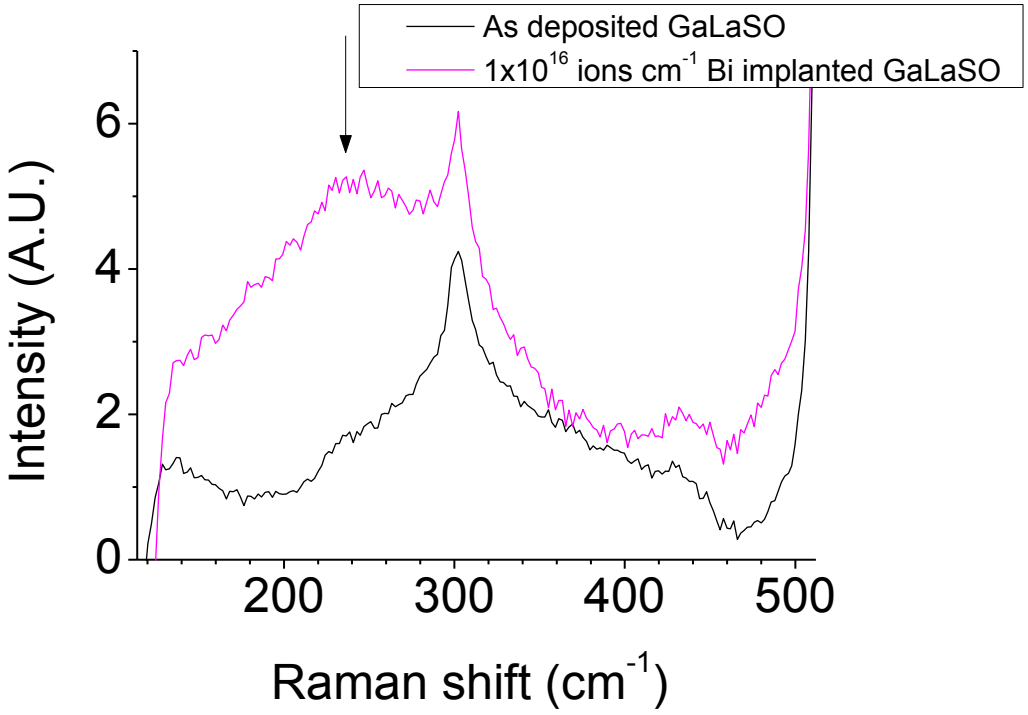

Supplementary Figure 4. Raman spectra of unimplanted and 1×10^{16} ions cm^{-2} Bi-implanted 100 nm thick GaLaSO film on thermal SiO_2/Si substrate, excited at 633 nm. A band at 235 cm^{-1} can be observed (indicated by the arrow) which has been attributed to the breathing mode of GaS_4 tetrahedra.[4] The narrow peak at 300 cm^{-1} is due to the Si substrate.

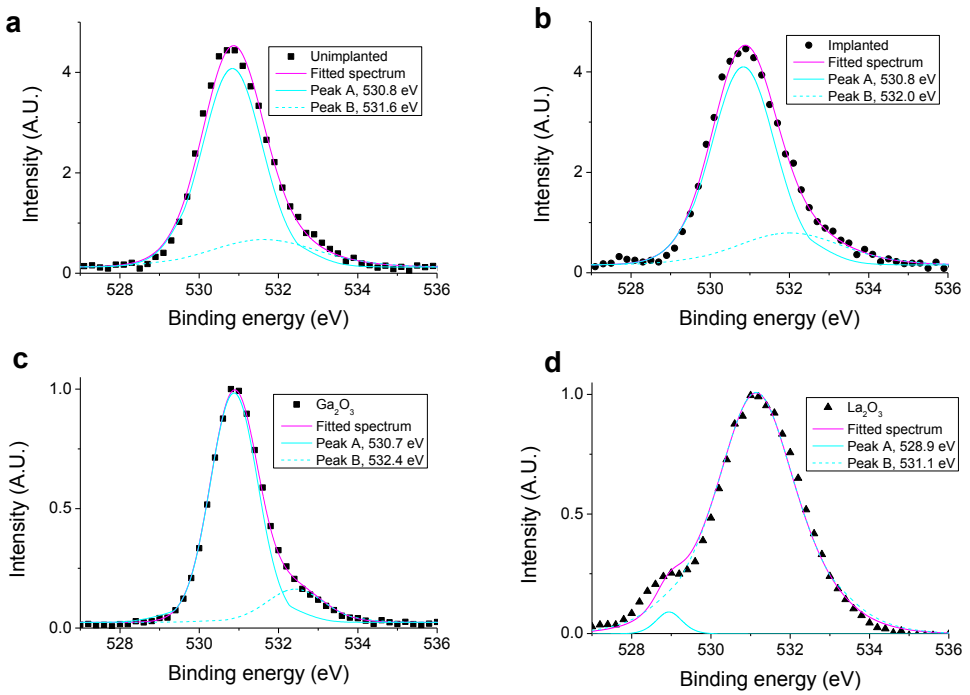

Supplementary Figure 5. Deconvolution into fitted Gaussian-Lorentzian peaks of the X-ray photoelectron spectroscopy (XPS) spectra of the O 1*s* level from the unimplanted (a) and implanted (b) region from a 1×10^{16} ions cm^{-2} Bi-implanted 200 nm thick GaLaSO film. The deconvolution into Gaussian-Lorentzian peaks shows a primary peak (peak A) at 530.8 eV, with a shoulder represented by peak B at 532.3 eV. After implantation, the relative intensity of peak B increases. Comparing the O 1*s* XPS spectra of GaLaSO to those of β-Ga_2O_3 (c) and La_2O_3 (d) shows that the primary O 1*s* peak in GaLaSO is in close agreement with the primary peak of both β-Ga_2O_3 and La_2O_3. We can therefore attribute it to either Ga or La coordinated O, although we expect O to be mainly coordinated to La, based on the XPS spectra of the Ga, La and S in Supplementary Figure 3, 7, and 8. The O 1*s* binding energy is slightly higher in La_2O_3 than it is in β-Ga_2O_3; however, the higher binding energy peak B in GaLaSO, which increases after implantation, cannot be attributed to any modification of the La-O network in GaLaSO because the XPS spectra of La 3*d* levels in Supplementary Figure S7 show that there is no change after implantation. Peak B of β-Ga_2O_3 is a good match to

peak B in GaLaSO; however, a similar peak has been observed in β-Ga_2O_3 and attributed to hydroxide impurities.[5] It is conceivable that hydroxide impurities could increase after implantation through the secondary implantation of any hydroxide impurities that may exist on the surface of the film, but these should be restricted to a monolayer, and 'transport of ions in matter' (TRIM) computer simulations indicate that less than 1% of such a hydroxide monolayer would undergo secondary implantation and would be restricted to the top 20 nm of GaLaSO. Another possibility is the formation of homopolar O-O bonds after implantation which would be expected to have a higher binding energy than Ga-O and La-O bonds because of the significantly higher electronegativity of O and which could account for peak B in GaLaSO. However, no reference standard materials are available for O-O bonds. The absorption spectrum in Supplementary Figure 9 indicates that homopolar bonds could be formed. XPS measurements of Ga and La core levels in Supplementary Figure 3 and 7 indicate that no Ga-Ga or La-La homopolar bonds are formed after implantation; therefore, only S-S or O-O wrong bonds could be formed. Homopolar O-O may exist as an interstitial O_2 molecule in a similar manner to N_2 in phase-change chalcogenides,[6,7] but this would make a change in the bandgap unlikely. It is possible that O species could exist in the GaLaSO network that have a different Ga coordination than in β-Ga_2O_3. The structure of β- Ga_2O_3 consists of zigzag double chains of edge-sharing GaO_6 octahedra, linked by single chains of vertex-sharing GaO_4 tetrahedra,[8] with different O sites that are either 3 or 4-fold coordinated to Ga.[9] Ga_2O_3 can also exist in a hexagonal α-phase which has a corundum structure with O 4-fold coordinated to Ga and can be obtained at high temperatures and pressures.[8] α-Ga_2O_3 has a higher O 1*s* binding energy than β-Ga_2O_3, whereas the Ga binding energy is lower.[10] We therefore propose that the most likely explanation for peak B in GaLaSO is an O species in an environment similar to α-Ga_2O_3, whereas peak A can be attributed to both an O species in an environment similar to β-Ga_2O_3 and a La-coordinated O species with a similar La

coordination to La_2O_3. This indicates two Ga_2O_3 phases exist in GaLaSO (α and β). The O 1*s* level of the α-Ga_2O_3-like phase can be observed to increase after implantation, whereas the Ga $2p_{3/2}$ level of the β-Ga_2O_3-like phase can be observed to decrease after implantation. The O 1*s* level of the β-Ga_2O_3-like phase and the Ga $2p_{3/2}$ level of the α-Ga_2O_3-like phase are expected to occur at lower binding energies and are therefore obscured by the primary peaks of the XPS spectra.

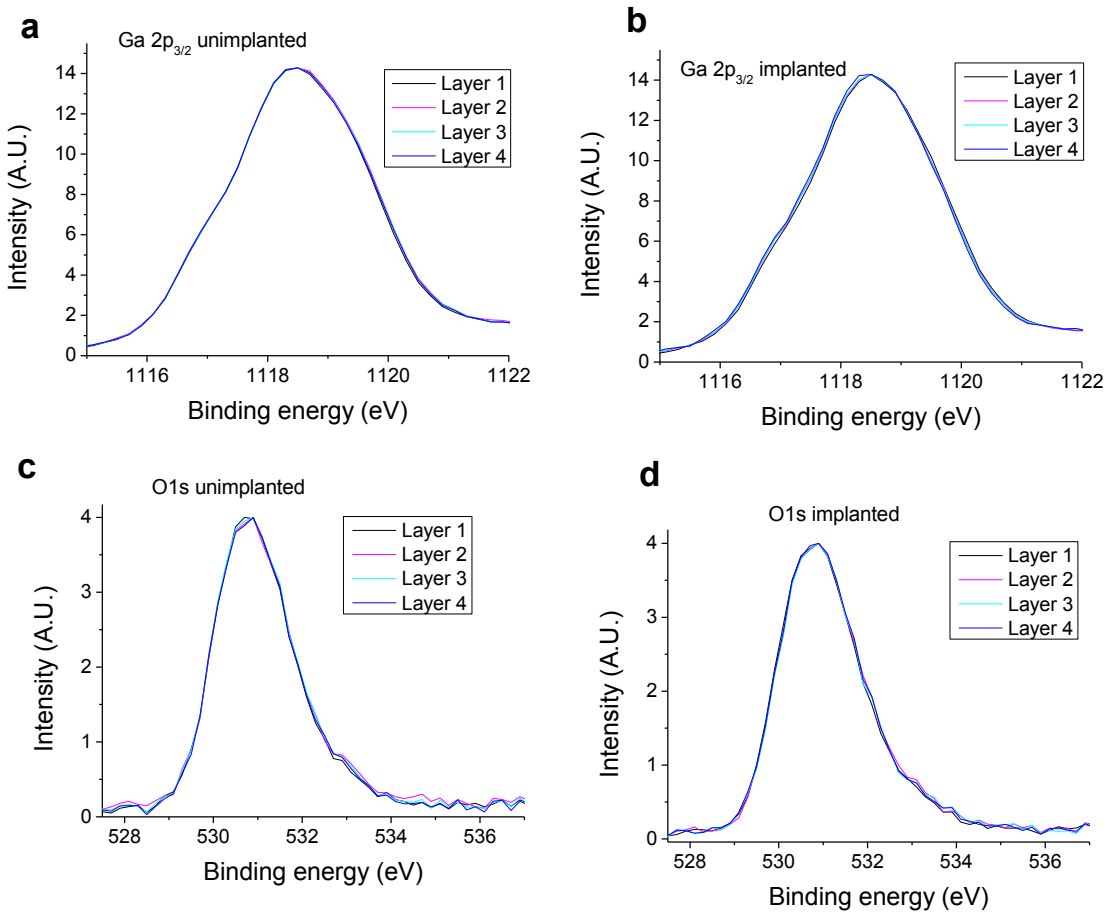

Supplementary Figure 6. X-ray photoelectron spectroscopy (XPS) measurements indicating the significance of the differences between implanted and unimplanted regions observed in Figure 3 by showing the similarity of various etch levels from within the same region. Ga $2p_{3/2}$ level from the unimplanted region (a) and Bi-implanted region (b). O1*s* level from the unimplanted region (c) and Bi-implanted region (d). Three standard deviations in intensity for the four layers measured for each species was 0.6% for Ga and 2.4% for O. The maximum difference in intensity observed in Figure 3 was 7.7% for Ga and 30% for O. So the differences observed in Figure 3 are over an order of magnitude greater than is accounted for by variation in the measurement.

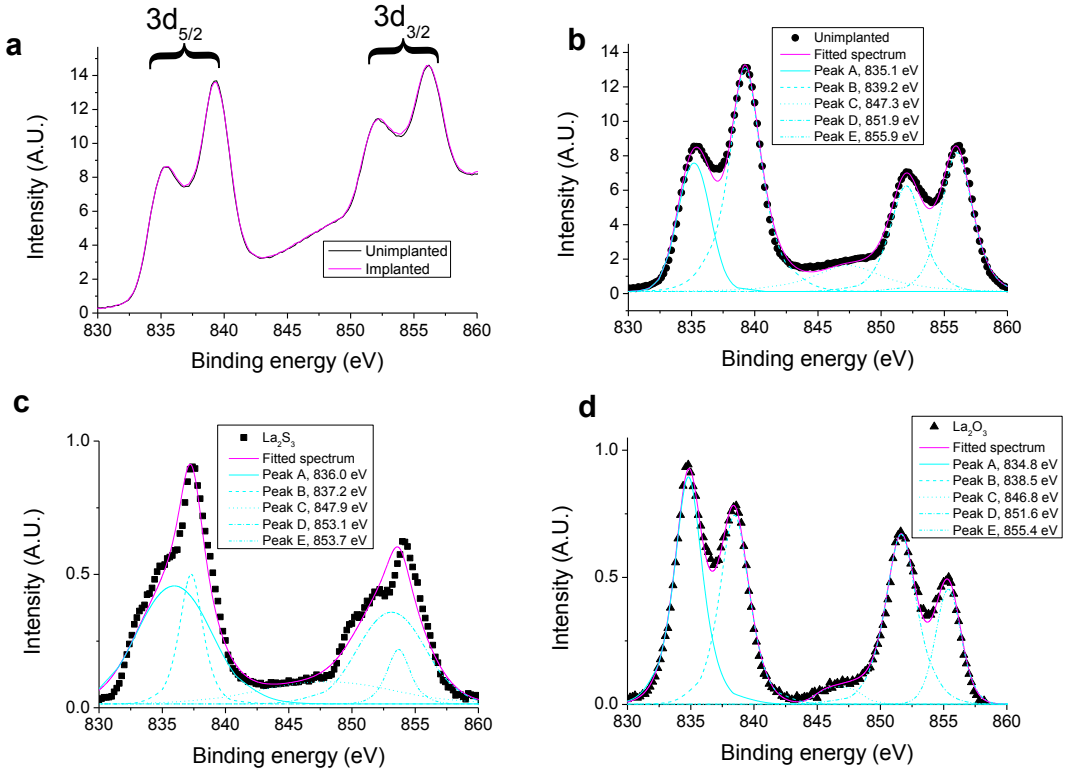

Supplementary Figure 7. (a) X-ray photoelectron spectroscopy (XPS) spectra of the La $3d_{5/2}$ and $3d_{3/2}$ levels from the Bi-implanted and unimplanted regions of the 200 nm thick GaLaSO film. Both the $3d_{5/2}$ and $3d_{3/2}$ levels display satellite peaks at higher binding energies due to simultaneous transfer of a ligand electron to the empty 4*f* shell during X-ray photoionisation.[11] There is essentially no observable difference in the La XPS spectra in the implanted and unimplanted regions. Deconvolution into Gaussian-Lorentzian peaks of the XPS spectra from the unimplanted region of GaLaSO film (b), La_2S_3 crystalline powder (c) and La_2O_3 crystalline powder (d). For simplicity of comparison, we have fitted one Gaussian-Lorentzian satellite peak, although more than one can be fitted in various La compounds.[12,13] The primary peaks, A and D, correspond to the $3d_{5/2}$ and $3d_{3/2}$ states, respectively, without a charge-transfer process.[13] The satellite peaks B and E represent the $3d_{5/2}$ and $3d_{3/2}$ states, respectively, with a simultaneous charge transfer.[13] Peak C corresponds to the plasmon loss peak.[14] The XPS spectra of Ga in GaLaSO show no evidence of Ga-La bonds and La is only

likely to be bonded to O or S in the GaLaSO network; therefore, comparison of GaLaSO spectra to those of the oxide and sulphide crystalline compounds can indicate which bonds predominate in the network. This comparison shows a significantly closer correspondence of GaLaSO with La_2O_3 than with La_2S_3, which indicates that La is mostly coordinated with O. The primary $3d_{5/2}$ and $3d_{3/2}$ levels are both 0.3 eV higher in GaLaSO than in La_2O_3, which is close to the 0.2 eV resolution of the XPS spectrometer. The poor fit in the La_2S_3 spectrum indicates that more satellite peaks are present.

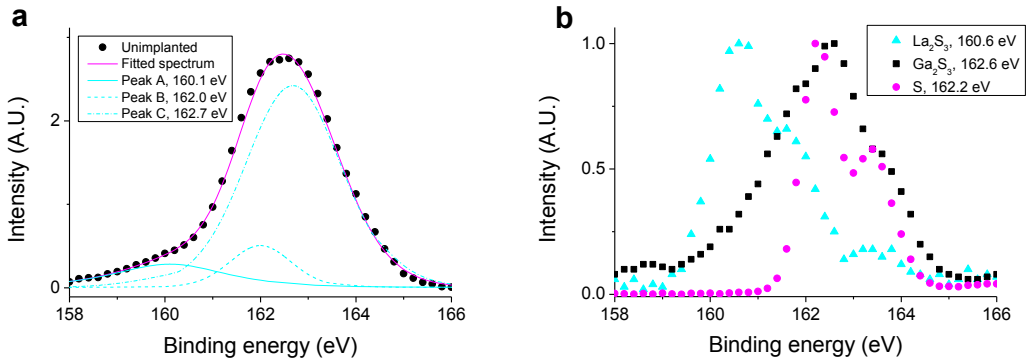

Supplementary Figure 8. (a) Deconvolution into fitted Gaussian-Lorentzian peaks of the S 2*p* X-ray photoelectron spectroscopy (XPS) spectrum from the unimplanted region of the 200 nm thick GaLaSO film. The implanted region cannot be analysed because of the overlap of the Bi $4f_{5/2}$ level with the S 2*p* level. (b) XPS spectra of the S 2*p* level in La_2S_3, Ga_2S_3 and S (α-S_8) crystalline powders. In La_2S_3 and S, the spin-orbit splitting into the low binding energy S $2p_{3/2}$, and high binding energy S $2p_{1/2}$ levels can be resolved. The weak tail in the S 2*p* peak in GaLaSO (peak A) corresponds well with the peak binding energy of the S 2*p* peak in La_2S_3, whereas the primary peak corresponds with both Ga_2S_3 and S. This supports the finding from the XPS spectra of the La 3*d* levels in Supplementary Figure 7 which indicated that La is predominantly coordinated with O. The primary S 2*p* peak in GaLaSO can be fitted well with two Gaussian-Lorentzian peaks (B and C) which correspond to the S 2*p* binding energy of S and Ga_2S_3, respectively. The relative magnitude of these peaks indicates that S is predominantly coordinated to Ga, which is supported by the Ga XPS spectra in Supplementary Figure 3 and the Raman measurements in Supplementary Figure 4. It also indicates that a small proportion of homopolar S-S bonds is present, which is supported by the absorption measurements in Supplementary Figure 9.

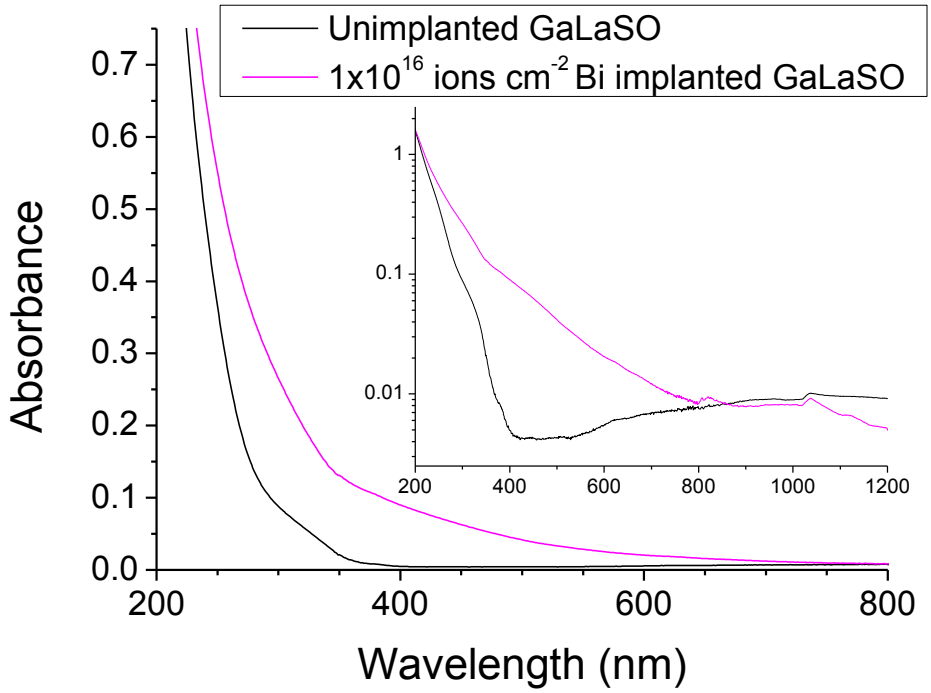

Supplementary Figure 9. Absorption spectra of unimplanted and 1×10^{16} ions cm^{-2} Bi-implanted 100 nm thick GaLaSO films deposited on fused silica substrates. The inset shows a log scale. Absorbance spectra, $A(\lambda)$, were calculated from % transmittance, $T(\lambda)$, and % reflection, $R(\lambda)$, spectra using $A(\lambda) = 2\text{-}\log(T(\lambda)+R(\lambda))$; for longer wavelength regions where $T(\lambda)+R(\lambda) \approx 100\%$, for $T(\lambda)+R(\lambda) <\sim 100\%$, we obtained the absorbance spectra using $A(\lambda) = 2\text{-}\log(T(\lambda))$. There was a good agreement in the overlapping spectral region between the two expressions. Homopolar bonds and bond-angle disorder give rise to states near the valence- and conduction-band edges, which result in a reduction of the optical band-gap energy and a red-shift in the absorption edge.[15] A red-shift in the band edge of GaLaSO after Bi implantation can be observed, in line with this expectation. There is also a significant red-shift in the Urbach edge which is related to disorder[15] and the breaking and weakening of bonds between non-bonded chalcogen atoms in neighboring layers (intermolecular bond breaking).[16] XPS measurements in Supplementary Figure 3 indicate no homopolar Ga-Ga bond formation after implantation; we therefore attribute the red-shift in the absorption band to S-S homopolar bond formation.

Supplementary references

1 Moulder, J. F. & Chastain, J. *Handbook of X Ray Photoelectron Spectroscopy: A Reference Book of Standard Spectra for Identification and Interpretation of Xps Data*. Pg 90 (Physical Electronics Division, Perkin-Elmer Corporation, 1995).

2 Crist, B. V. *Handbook of Monochromatic XPS Spectra, The Elements of Native Oxides*. Pg 374 (Wiley, 2000).

3 Wolter, S. D. *et al.* X-ray photoelectron spectroscopy and x-ray diffraction study of the thermal oxide on gallium nitride. *Appl. Phys. Lett.* **70**, 2156-2158 (1997).

4 Flahaut, J., Guittard, M. & Loireau-Loozac'h, M. Rare earth sulphide and oxysulphide glasses. *Glass Technol.* **24**, 149-156 (1983).

5 Al-Kuhaili, M. F., Durrani, S. M. A. & Khawaja, E. E. Optical properties of gallium oxide films deposited by electron-beam evaporation. *Appl. Phys. Lett.* **83**, 4533-4535 (2003).

6 Kim, Y., Baeck, J. H., Cho, M.-H., Jeong, E. J. & Ko, D.-H. Effects of N^{2+} ion implantation on phase transition in $Ge_2Sb_2Te_5$ films. *J. App. Phys.* **100**, 083502 (2006).

7 Ki-Hong, K. *et al.* Nitrogen-Doping Effect on $Ge_2Sb_2Te_5$ Chalcogenide Alloy Films during Annealing. *Jpn. J. Appl. Phys.* **49**, 101201 (2010).

8 He, H. Y. *et al.* First-principles study of the structural, electronic, and optical properties of Ga2O3 in its monoclinic and hexagonal phases. *Phys. Rev. B* **74**, 195123 (2006).

9 Bermudez, V. M. The structure of low-index surfaces of b-Ga2O3. *Chem. Phys.* **323**, 193-203 (2006).

10 Reddy, B. M., Ganesh, I., Reddy, E. P., Fernández, A. & Smirniotis, P. G. Surface Characterization of Ga_2O_3−TiO_2 and V_2O_5/Ga_2O_3−TiO_2 Catalysts. *The Journal of Physical Chemistry B* **105**, 6227-6235 (2001).

11 Jørgensen, C. K. & Berthou, H. Split photo-electron signals from the unique closed-shell cation lanthanum(III). *Chem. Phys. Lett.* **13**, 186-189 (1972).

12 Talik, E., Novosselov, A., Kulpa, M. & Pajaczkowska, A. Electronic structure of La 3d in gallate and aluminate single crystals. *J. Alloy. Compd.* **321**, 24-26 (2001).

13 Sunding, M. F. *et al.* XPS characterisation of in situ treated lanthanum oxide and hydroxide using tailored charge referencing and peak fitting procedures. *J. Electron Spectrosc. Relat. Phenom.* **184**, 399-409 (2011).

14 Park, K. H. & Oh, S. J. Electron-spectroscopy study of rare-earth trihalides. *Phys. Rev. B* **48**, 14833-14842 (1993).

15 Asal, R. & Rutt, H. N. Optical properties of laser ablated gallium lanthanum sulphide chalcogenide glass thin films prepared at different deposition laser energy densities. *Opt. Mater.* **8**, 259-268 (1997).

16 Elliott, S. R. A unified model for reversible photostructural effects in chalcogenide glasses. *J. Non-Cryst. Solids* **81**, 71-98 (1986).